Autophagy modulation in head and neck squamous cell carcinoma cell lines: a new target for cancer treatment

Javier Fernández-Mateos, María Ovejero-Sánchez, Pedro Blanco Pérez, Ángel Muñoz Herrera, Juan Luis García Hernández, Juan Jesús Cruz-Hernández, Rogelio González-Sarmiento

Molecular Cancer Therapeutics

Sometido a publicación

Factor de impacto 2015: 5.579

-Journal Citation Reports Science Edition (Thomson Reuters, 2015)

Oncology: 27/213 Q1

6

Artículo 6: "Autophagy modulation in head and neck squamous cell carcinoma cell lines: a new target for cancer treatment"

El uso de moduladores de la autofagia está emergiendo como una diana potencial para la terapia del cáncer. La combinación de modificadores autofágicos con un agente quimioterápico ha demostrado efectos sinérgicos. A pesar de la gran variedad de combinaciones de terapias empleadas en el CECC, la supervivencia a los 5 años no ha demostrado grandes cambios. Por ello, nos proponemos el estudio de fármacos y su modulación en la autofagia como nueva vía de tratamiento en líneas comerciales y establecidas de CECC de diferentes localizaciones con el propósito de definir una terapia antitumoral novedosa que mejore las pobres tasas de respuesta observadas en los CECC.

Tras el establecimiento de tres líneas celulares obtenidas de biopsias quirúrgicas de tumores de laringe (32860), valécula (32816) y orofaringe HPV+ (32816) y el uso de la línea comercial CAL33 como representativa de tumores de cavidad oral, éstas se caracterizaron tanto a nivel morfológico (H&E) como a nivel molecular mediante el estudio de variaciones en el número de copias y cariotipado. Posteriormente, se realizó un ensayo de análisis de fármacos en dos etapas: viabilidad celular mediante MTT y ciclo celular por citometría de flujo. El análisis de la autofagia se estudió mediante western-blot de las proteínas fosfo-mTOR, p62, beclin1 y LC3B. Se emplearon los fármacos cloroquina, decitabina, metformina, paclitaxel y panobinostat.

Aunque se observaron algunas diferencias en el fenotipo, todas las líneas celulares presentaron características epiteliales. Los resultados de caracterización permitieron confirmar las diferencias moleculares entre las distintas localizaciones tumorales de las líneas celulares, a pesar de que estas diferencias fueron mayores en el cariotipo que en el número de variación de copias, donde se asemejaban a la descripción general surgida de la caracterización de diferentes líneas celulares de CECC.

La adición de tratamientos mostró una disminución en la viabilidad celular dosis-dependiente, excepto en el caso de la decitabina, sin efecto en la proliferación celular. Esto permitió definir las concentraciones óptimas de 25µM de cloroquina, 7.5 µM de decitabina, 8mM de metformina, 10nM de paclitaxel y 50nM de panobinostat para los estudios posteriores de citometría y extracción de proteínas.

A pesar de las variaciones entre las diferentes líneas celulares utilizadas, globalmente el estudio del ciclo celular mostró cómo el inhibidor autofágico cloroquina, agente lisosomotrópico, producía una parada en G0/G1, con una disminución de G2/M y un pequeño incremento en la muerte celular. La cloroquina produjo un aumento en la expresión de p62 y una disminución de las proteínas específicas de autofagia (beclin1 y LC3B).

Por el contrario, el inhibidor de histona deacetilasas e inductor de la expresión génica de la vía autofágica decitabina, produjo un descenso en G0/G1 con un aumento en fase S y muerte. El análisis de proteínas corroboró el aumento de autofagia por sobreexpresión de las dos proteínas específicas estudiadas.

El resultado con metformina, fármaco antidiabético con propiedades antitumorales e inhibidor de autofagia mediante la inhibición de mTOR, mostró los resultados más llamativos con un descenso en G0/G1 y un aumento en fase S y en G2/M. El tratamiento produjo una gran disminución de los niveles de fosfo-mTOR, produciendo un aumento leve de LC3B-II.

La adición de paclitaxel, principio activo utilizado para el tratamiento de CECC, inhibidor de la formación de microtúbulos y por lo tanto del transporte de las vesículas autofágicas, obtuvo el mayor efecto citotóxico con una media de muerte del 35%, excepto en la línea de laringe 32860, que parece más resistente al paclitaxel. El efecto en la autofagia de esta droga no fue uniforme según la línea celular con un aumento leve de beclin1 y LC3B-I.

Por último, el inhibidor de histonas deacetilasas panobinostat produjo una disminución en G0/G1 y un importante incremento en G2/M, produciendo también un pequeño aumento en muerte celular. Al igual que en los ensayos de viabilidad celular, la línea celular 32816 tuvo un comportamiento diferente, con mayor sensibilidad a todos los tratamientos e inducción uniforme en la expresión de beclin1 y LC3B en todas las líneas celulares.

Este análisis preclínico confirma la utilidad de fármacos moduladores de autofagia en el tratamiento de CECC ya sea como monoterapia o en poliquimioterapia. Esta sinergia parece ser más apropiada en tumores HPV+, puesto que las líneas celulares derivadas de este tipo tumoral han resultado más sensibles al tratamiento.

Autophagy modulation in head and neck squamous cell carcinoma cell lines: a new target for cancer treatment

Javier Fernández-Mateos[1,2,3,4], María Ovejero-Sánchez[3], Pedro Blanco Pérez[2,5], Ángel Muñoz Herrera[2,5], Juan Luis García Hernández[2,4], Juan Jesús Cruz-Hernández[1,2,3,4,], Rogelio González-Sarmiento[2,3,4,*]

[1]Medical Oncology Service, University Hospital of Salamanca-IBSAL, Salamanca, 37007 Spain

[2]Biomedical Research Institute of Salamanca (IBSAL), SACYL-University of Salamanca-CSIC, Salamanca, 37007, Spain.

[3]Molecular Medicine Unit- IBSAL, Department of Medicine, University of Salamanca, 37007, Spain

[4]Institute of Molecular and Cellular Biology of Cancer (IBMCC), University of Salamanca-CSIC, Salamanca, 37007, Spain

[5]Othorhinolaryngology Department, University Hospital of Salamanca-IBSAL, Salamanca, 37007 Spain

Abstract

Head and neck squamous cell carcinomas (HNSCC) are treated with multidisciplinary options but their survival rates remain limited. Autophagy pathway has a dual role in carcinogenesis and its use as therapeutic target could define a new treatment alternative that could improve the outcomes in HNSCC. In this study four cell lines from different locations (laryngeal, pharyngeal, tongue and vallecula tumours) were used for autophagy modulation drug screening. Three of these cell lines were newly established and characterized, showing molecular and phenotypic differences between them. Chloroquine, decitabine, metformin, paclitaxel and panobinostat were tested by MTT cell viability assay, cell cycle analysis by flow cytometry and autophagy expression by western blot of phospho-mTOR, p62, beclin1 and LC3B proteins. The results showed that paclitaxel, chloroquine and panobinostat were the most effective drugs in HNSCC cell line viability and cell cycle modification, reaching paclitaxel the highest death rates. Moreover, all treatments showed a modification of autophagy proteins expression in different ways. Differences between tumour locations were notable between cell lines and confirm the diversity in HNSCC. In conclusion, autophagy modulation could be a promising target therapy especially in HPV positive HNSCC, because of the highest sensibility in the HPV+ tumour derived cell line.

Keywords: Head and neck cancer, drug screening, autophagy, cell lines, establishment

Introduction

Head and neck squamous cell carcinoma (HNSCC) includes epithelial malignancies of the oral cavity, pharynx and larynx[1]. It is the sixth most common tumour with an incidence of 600.000 cases per year worldwide[2]. Most important risk factors are tobacco and alcohol consumption, although virus infection, mainly human papillomavirus (HPV), is also an important etiological cause[3] defining a different molecular entity than caused by tobacco and alcohol. HNSCC treatment options comprise a multidisciplinary approach including surgery or/and radiotherapy for early-stages, whereas locally advanced tumours also include chemotherapy (induction chemotherapy and/or chemoradiation) and biotherapy[4]. Disappointingly, 5-years survival rates remain below 50%, without a significant improve in the last decade[5].

Most common events along HNSCC development have been described[5]. These tumours usually have complex karyotypes with frequent copy number gains on 3q, 8q, 9q, 11q and 20q chromosomal arms, as well as losses of 3p, 4q, 9p and 18q[6–8]. Moreover, genetic alterations in HNSCC are abundant and include lot of different pathways[9], being classified according to their expression profiles in different groups[10]. HNSCC cell lines are good preclinical models to test novel treatment therapies. In spite of more than 300 HNSCC cell lines reported[11], most of them did not come from the primary tumour site and molecular characterization and clinical features are not available.

Macroautophagy (referred from now as autophagy) is one of the most conserved cellular degradation pathway[12]. Its role in cancer is controversial, acting both in promotion and inhibition of the tumourigenesis[13]. Alterations in autophagic signaling pathways are frequently observed in cancer[13], so the use of autophagy modulators is emerging as a potential target for cancer therapy[14]. The combination of autophagy modifiers with a chemotherapy agent has shown benefits in treatment effects[15]. Although molecular process of autophagy is well described[16], understanding its role in cancer, may allow us to develop novel therapeutic strategies to enhance the effects of chemotherapy and improve the clinical outcome of cancer patients[17]. Certain proteins status such as conversion from LC3B-I to LC3B-II, phospo-mTOR and p62 down-regulation and Beclin-1 increase are considered the best indicators of active autophagy[18].

The purpose of this article was to study the use of some drugs and the autophagy modulation in commercial and new established molecularly characterized HNSCC tumour cell lines from all the main locations, to check their effect in viability and cell cycle modification. Alteration in autophagy protein expression was also studied to show the real effect of inducers or inhibitors in this pathway. This could define a promising novel cancer therapy, improving the poor response rates observed in HNSCC tumours.

Material and methods

Cell lines establishment and culture conditions

Surgically resected fresh HNSCC tumour biopsies from Othorhinolaryngology operating theatre were received in aseptic conditions, after signed informed consent by the patient. After three

washes with phosphate-buffered saline (PBS) + 1% penicillin and streptomycin (Gibco, Life Technologies, Carlsbad, CA) + 1% amphotericin B (Sigma-Aldrich, St. Louis, MO), pieces were cultured in a dish with enriched RPMI 1640 medium with 20% heat-inactivated fetal bovine serum (FBS) (Gibco-Life Technologies, Carlsbad, CA) + 2% penicillin/streptomycin. After mechanical degradation by tumour extrusion in the dish, they were incubated at 37ºC in a 5% of CO_2 atmosphere. Tumour cells were purified by removal of fibroblast in sequence passages. Cells were passaged twice a week by trypsinization and the tumour cell line was considered established after 30 passages. Finally from nine different tumours, we established three different squamous cell carcinomas cell lines from oropharyngeal (32816), laryngeal (32860) and vallecula, the region between pharynx and larynx (32661).

Because of the lack of an oral cavity tumour cell line, CAL33 from human tongue squamous cell carcinoma was purchased from American Type Culture Collection (ATCC, Rockaville, MD) and was cultured under the same conditions described above.

Cell lines characterization

Characterization of the different cell lines was done in different steps. First of all, trypsinized cells were fixed in 70% methanol and centrifuged in the cytospin. Hematoxylin and eosin staining was done in the slides to corroborate their tumourogenicity phenotype.

Cytogenetic analysis and FISH procedure

Chromosome preparation were processed as previously described[19]. Briefly, before harvesting, HNSCC cells in the logarithmic growth phase were incubated with 100 ng/ml colcemid (Gibco-Life Technologies, Carlsbad, CA) for 45 min. The cells were harvested by treatment with 0.025% trypsin-EDTA, suspended in 0.075 MKCl at room temperature for 20 min, and fixed with methanol/ acetic acid (3:1) three times. Chromosomes were identified by G-banding and karyotypes were described according to the ISCN, 2016[20]. Dual color FISH using Vysis whole chromosome painting (WCP) probes, a chromosome 1 painting probe (WCP 1) labelled in SpectrumOrange and chromosome 3 painting probe (WCP 3) labelled in SpectrumGreen (Abbott Molecular, VYSIS, Chicago, IL) were prepared according to the manufacturer's instructions.

Affymetrix CytoScan 750K

DNA was extracted from cell line using the QiaAmp DNA Mini Kit (Qiagen, Hilden, Germany) and analysed on the Affymetrix® CytoScan 750K Array according to the manufacturer's protocol (Affymetrix, Santa Clara, CA). The CytoScan 750K Array provides whole-genome coverage, with more than 750,000 markers for copy number analysis and over 200,000 SNPs for genotyping. Data analysis was performed using the Chromosome Analysis Suite (CHAS) (Affymetrix, Santa Clara, CA). All markers were used to determine copy number and SNP probes were used to calculate loss of heterozygosity (LOH) and genotype.

Cell viability assay

$10x10^3$ cells were seeded on a 24 well plate and were treated with a battery of autophagy modulators such as: Panobinostat, Decitabine, Chloroquine, Paclitaxel and Metformin.

Concentrations of the drugs are indicated in table 1. Treatments were done for 72 hours, measuring each 24 hours the viability of the cells by cellular metabolic function using 3-(4,5-dimethylthiazol-2-yl)-2,5-diphenyl-2H-tetrazolium bromide (MTT) (Sigma-Aldrich, St. Louis, MO; 98% purity). MTT salt dissolved in PBS, pH7.2, at 5mg/ml was added to the cells (110ul/well). MTT was reduced via mitochondrial dehydrogenases converting into formazan. After incubation at 37ºC for 1 hour, the medium was aspirated. The formazan crystals were dissolved in 500ul of dimethylsulfoxide (DMSO) and the absorbance was measured at 570nm in a plate reader (Ultra Evolution, Tecan, Mannedorf, Switzerland). Blank and control without drugs were always used. All the experiments were performed in triplicate and were repeated at least three times under the same conditions. Curves of viability were calculated subtracting the background of the blank and converting the absorbance of the tetrazolium salt absorbance in terms of percentage respect to the control. Optimal concentrations were calculated according to the minimum inhibitory concentration in all the cell lines.

Flow cytometry

In order to analyze the effect on the cell cycle induced by selected drugs, flow cytometry was performed with the optimal concentration calculated by the viability assays. Cells were treated again for 72 hours and both supernatant and trypsin treated adherent cells in treated and controls were taken each 24 hours, 70% cold ethanol fixed and store at -20ºC until the last day. Last day, ethanol was removed by sequence of washes with PBS and finally they were resuspended in 1ml of PBS, stained with 50µg/ml propidium iodide (PI) (Sigma-Aldrich, St. Louis, MO) and treated with 100µg/ml RNase, to removed RNA. After an overnight incubation at room temperature, 30.000 cells cycle was measured in FACScalibur flow cytometer (BD Biosciences, San Jose, CA). DNA histogram of cytometry data was analyzed in the CellQuest Pro software (BD Biosciences, San Jose, CA) and cell cycle phase percentage was calculated in WinMDI 2.9 software (Windows, Albuquerque, NM).

Protein extraction and western blot

Cells were collected with trypsin each day for 72 hours after treatment at specific concentrations. After 45 minutes incubation with cell lysis buffer on ice, lysates were centrifugated at 15000rpm during 15 minutes at 4ºC and recovered protein supernatants measured in spectophotometry (Nanodrop) at 260nm. 50ug of proteins were separated in 8% and 12% SDS-PAGE at 120V and immunoblotted with specific antibodies against LC3B (Novus, ref.NB600-1384, 1:1000) Beclin-1 (Cell signaling, ref. 3738S, 1:1000), p62 (Abcam, ref.ab109012, 1:1000) and mTOR (Cell Signalling, ref.2972S, 1:1000) in transferred polyvinylidene difluoride (PVDF) membranes (GE Healthcare, Barcelona, Spain). Membranes were incubated with the corresponding horseradish peroxidase-conjugated (HRP) secondary antibody at 1:10000 (Santa Cruz Biotechnology, CA) and were developed using Pierce® ECL Western Blotting substrate (Thermo Scientific, Madrid, Spain). Developed signals were recorded on X-ray films (Fujifilm Spain, Barcelona, Spain).

Statistical analysis

Statistic comparison with one variable (treated vs. untreated cell cycle phase each 24 hours) was performed using a Student's two-tailed, paired t test or one-way analysis of variance

(ANOVA). The difference was considered to be statistically significant when $p < 0.05$. Results are expressed as mean ± standard deviation (SD).

All these tests were conducted using SPSS software version 21.0 (SPSS Inc., Chicago, IL) and GraphPad Prism software version 6.0 (GraphPad Softare Inc., CA).

Results

Clinical features of the biopsies are described in Table 2. All the patients were high tobacco and alcohol consumers. Importantly, 32816 cell line was derived from a histologically confirmed HPV positive tumour by $p16^{INK4a}$ immunohistochemistry.

Cell lines characterization

HNSCC tumour tissues culture produced epithelial outgrowths with the typical cobblestone patterns. Lines were morphological distinct. 32661 had a nest-like growth pattern while the rest of the cell lines were more spread. 32860 culture showed two main morphological cell types (a low dense big stem cell-like phenotype that differentiates in regular epithelial phenotype cells), whereas 32816 grew as a very uniform culture and CAL33 had more filamentous aspect. H&E staining confirmed tumour morphology showing the presence of pleomorphic cells, with nucleus-cytoplasm disproportion, eosinophil dense cytoplasm and very irregular hyperchromatic nucleus with the presence of atypical mitosis (Supplementary figure S1).

Karyotyping of the cells lines by G banding revealed a moderate hyperploidy, with an average number of 47-49 chromosomes per cell, except for CAL33 that showed a near-tetraploidy karyotype. Cytogenetics analysis of the cells lines detected rearrangements involving chromosomes 3, 7, 8, 9, 18, 20 and X. These changes were described as 3p+, i(7q), i(8q), der(X), deletion of 18 and gains of 20. However, conventional cytogenetics showed genomic changes specific for cell lines. For example, in 32816 cell line FISH analysis demonstrated that part of chromosome 3 was translocated on chromosome 12, showed an unbalanced translocation between chromosome 12 and 3 (Figure 1). In 32661 cell line at least two different sub clones were observed. The loss of chromosome 4 was presented in two clones; however, only one of them showed der(18)t(18;?)(p11;?) (See Figure).

DNA copy number aberrations were detected in all HNSCC cell lines analysed. The median number of copy number aberrations for tumour cell line was 97. DNA copy number gains were more frequently detected (median: 49, range: 21–91) than losses (median 48, range: 12–112). The higher number of copy number aberrations was presented in CAL33 and 32661 cell lines. Data obtained from aCGH analyses are summarized in supplementary table S1.

In all cell lines the most frequently, minimal overlapping regions of copy number gain were found on 3q11.2-3q29, 7p22.3-7p11.2, 8q11.1-8q24.3, 9p24-p22.3, 9q21.13-9q22.32, 9q31.1-9q31.1, 16p13.2-p11.2, 20p13-q13.2, Xp22.2. Respect to copy number losses, minimal overlapping regions, were detected on 3p14.3-p21, 4q34.3-q35.1, 12q24.31, 16q22.1, 18q12, 18q21, 18q22.1-q23. In CAL33 cell line, losses on 5p/q, 21q21 and gains on 13q were also

detected. Losses on 2p25 and 2p22.3-2p14 were detected only in 32661 cell line (Supplementary figure S2).

Cell lines response to treatments

Most of the cells had similar growths rates with lower split ratios in 32816 and 32661 cell lines. Viability curves are represented in the figure 2. Although each cell lines presented small differences, globally, chloroquine treatment produced an important decrease in cell viability in all the concentrations, so 25µM minimum concentration was chosen for following experiments. On the contrary, decitabine did not show any pronounced viability decrease and we decided to use the highest concentration of 7.5µM. Between this opposite results we found the effects with metformin, paclitaxel and panobinostat, with a dose-dependent activity. In these experiments, minimum visible decreased viability concentration was chosen for the cytometry and protein expression analysis (8mM metformin, 10nM paclitaxel and 50nM panobinostat) (Table 1). The highest changes were observed in the cell line derived from laryngeal cancer (32860) and the one derived from HPV+ oropharyngeal tumour (32816) in which cells seem to have more viability than the rest.

After the treatment with the selected concentrations obtained by the MTT viability assay, cell cycle cytometry was performed (Figure 3). Mostly, comparing with the untreated controls, chloroquine treatment produced a slight increase in G0/G1, a little decrease in G2/M and a reduced increment in cell death. This data was most accused in 32816 HPV+ oropharyngeal cell line. On the contrary, decitabine caused a G0/G1 descent and a higher percentage in S and death phases. In metformin treatment the most visible result is a G0/G1 drop, resulting in S phase rise. Metformin produced a G0/G1 descent and consequently, an increase in S and G2/M phases, although in 32816 these effects were not found. Paclitaxel is the treatment option that showed the highest death rates, increasing respect the untreated control with an average of 35%, except in 32860 laryngeal cell line which seem to be more resistant to taxol. Lastly, panobinostat produced a diminished G0/G1 and an important increment in G2/M cell cycle phase, producing also a little cell death rise. Again, 32816 showed different results. All this results were statistically significant ($p<0.05$).

Western Blot analysis had similar tendency in protein expressions varying on the drug treatment in the four cell lines. Treatment with autophagy inhibitors such as chloroquine produced higher expression of p62 (except in 32816 where the expression was constant) and a slight decrease in beclin1 and LC3B, especially in LC3B-I. Regarding paclitaxel treatment, it did not follow a tendency, changing phospo-mTOR expression depending on cell type whereas the rest of the proteins were invariable or just a little descent in beclin and LC3B-I in 32816 cell line was observed. Autophagy inductors had different behavior in autophagy proteins expression. Treatment with decitabine altered phospo-mTOR and p62 expression depend on the cell line, but showed increased beclin1 in all cell lines and higher LC3B-II levels except in CAL33 and 32816 cell lines. On the contrary, metformin produced a strong inhibition of phospo-mTOR, reduced p62 expression except in 32661 and rise in LC3B expression with the exception of 32816. Lastly, panobinostat induced mTOR, beclin1 and LC3B up-regulation, effect shown in all the cell lines (Figure 4).

Discussion

Despite multi-modality therapy, HNSCC continues to have a 5-year survival of just over 50%. The search of new drugs to treat this illness remains critical to improve long-term survival. New therapeutic approaches based on autophagy in HNSCC could give us this new alternative to limited current treatments. For that reason, we selected five approved drugs to treat different diseases that can be implicated in the modulation of the autophagolysosome formation.

Characterization of cell lines showed the molecular differences between tumour locations although it was higher in karyotyping than CNV analysis. Array CGH of all cell lines revealed gains on 3q, 7p, 8q, 9p, 9q, 16p, and 20 and losses on chromosome 3p, 8p, 12q, and 18. These data were in good concordance with published data[8] from HNSCC cases available on www.progenetix.org[21]. In addition, the results of array CGH matched the described karyotype determined by conventional cytogenetics. Isochromosome 7p and 8q were clearly verified by DNA gains of 7p and 8q in array CGH. 8q gains and i(8q) were some of the most common structural and copy number alterations in HNSCC and have been previously reported many times in varied studies[22]. Although it is much less frequently reported in the literature, the related gain of 7p has already been found in HNSCC. The distal part of chromosomal arm 3q was another chromosomal region subject of DNA copy number present in the cell lines. These changes were previously found in HNSCC associated with adverse patients outcome[22]. Several candidate proto-oncogenes reside inside the minimal overlapping region 3q25-qter detected in our HNSCC cell lines. One of these proto-oncogenes is *PIK3CA*. The PI3K signalling pathway is involved in multiple cancer-related functions such as cell survival, proliferation and cell migration[22], as well as an important autophagy effector. An activation of this pathway was considered to play a crucial role in HNSCC tumourigenesis founding genomic amplification and consecutive high PIK3CA protein expression in precancerous dysplasias of HNSCC and in primary and metastatic oral squamous cell carcinomas[23]. Further attractive candidate oncogenes in this region, as *SEC62* and *SOX2,* have been shown to be overexpressed in HNSCCs, affecting the metastatic potential of cancer cells[24].

Chloroquine is one the most specific autophagy inhibitor[25]. It is a lysosomotropic agent able to pass through the lysosome membrane increasing the pH of the organule, preventing from cellular degradation and inhibiting autophagy. Its origin was as antimalarial agent although nowadays it is used for immunological, reumatic and skin diseases[14,26]. The incorporation of chloroquine in chemotherapy and radiotherapy regimens has showed antitumour capacity in different neoplasias, potentiating their effects[27]. Our results with 25µM chloroquine showed a slight increase in G0/G1, a little decreased in G2/M and a reduced increment in cell death. This result was also reported in different *in vitro* studies in which viability reduction was only detected from 20µM and increment in death only appeared at high doses, such as colon[28] and hepatocellular carcinoma[29] with the same effect on G0/G1 cell cycle arrest[30]. Moreover, chloroquine treatment showed an enhanced autophagy, may be a promising drug for cancer therapy.

Metformin, a biguanide, is commonly used as first-line oral treatment for type 2 diabetes mellitus. Although its mechanism of action is diverse, metformin, through AMPK induction, suppress mTORC1 activation and signaling[31], an important negative autophagy regulator[32]. Last decade, some epidemiological studies have identified an association between metformin treatment and lower risk to cancer development included HNSCC[33]. For that reason, some clinical trials have been proposed, showing treatment benefit as well[34]. Our results indicated that treatment with 8mM metformin produced a total inhibition of cell viability, similar to previous studies where metformin alone reduce cell viability in a dose-dependent manner[35]. Cell cytometry analysis showed a G0/G1 drop, resulting in S and G2/M phases rise. Different tumour cell lines treated with metformin proved a parade in G0/G1[36] and G2/M[37]. The difference between these results could be related with the concentration of the drug, because in other series metformin was used at higher concentrations and with prolonged treatment. Anyway, metformin treatment showed an autophagy rise in our cell lines, could being used in concomitation with other drugs against HNSCC.

In our HNSCC cell lines, paclitaxel showed an important increment in cell death. The active ingredient obtained from *Taxus brevifolia* targets microtubule formation, important in processes of cellular structure maintain, motility and vesicle transport through cytoplasm[38]. Inhibiting microtubules disassembly, paclitaxel promotes G2/M arresting, favouring apoptosis[39]. Our results corroborate this effect, also defined in other HNSCC series with similar concentrations[39]. This drug has a high antitumour potential, being accepted in the use of different neoplasias, among them in HNSCC. In HNSCC combination taxol with platin and 5-fluorouracil (known as TPF) is the best induction chemotherapy regimen for locally advanced tumours[40]. Apart from apoptosis induction, paclitaxel regulates another programmed cell response such as autophagy through two different mechanisms: inhibition of autophagosome formation and trafficking[41]. However, autophagy protein expression did not show important alterations due to paclitaxel, maybe because of the main effect in apoptosis. So, the interplay between taxane treatment, autophagy and cell death should be taken into account as novel therapeutic implication of this widely used chemotherapy agent.

During tumourigenesis, many of the changes in gene expression are due to an altered epigenetic regulation such as DNA methylation and histone deacetylation[42]. Histone deacetilases (HDACs) are enzymes that regulate genetic expression through the removal of acetyl groups from lysines residues of histones producing a condense chromatin state and genetic silencing[43]. Panobinostat (LBH 589) is a potent pan-inhibitor of histone deacetilase class I, II and IV. Panobinostat acts through different pathways, allowing expression of tumour suppressor genes between others, causing an antiproliferative activity. It has been approved for some neoplasias, mainly in multiple myeloma[44]. HDACs inhibitors suppress cell proliferation by activation of cell-cycle checkpoints at G1/S or G2/M[44]. In our study it caused cell proliferation inhibition at 50mM, producing a G2/M arrest and cell death. This result has been reported in other *in vitro* studies like HNSCC[45]. Autophagy induction by HDACi was also described[46] as it was observed in our cell lines with an important autophagy stimulation after treatment with panobinostat.

DNA hypermethylation, by DNMTs, is one of the most studied epigenetic mechanisms in cancer[47]. So, the application of DNMTs inhibitors is a good therapeutic tool for cancer,

including HNSCC. Decitabine (5-aza-2´-deoxicitidine) is a cytidine analogue which inhibit DNMTs preventing the methylation[48]. Because decitabin incorporates during the synthesis, is it a specific S phase agent, as we showed in our results where decitabine produced a fall in G0/G1 and a higher percentage in S and death phases. Its use has been approved for myelodysplastic syndromes and acute myeloid leukemia[49]. However, decitabine is commonly used in combination of chemotherapy or radiotherapy, enhancing the effects of this treatments[50]. That could be explained the poor effects on the viability assay, where decitabine did not produced a decrease in cell viability. However, decitabine treatment caused an effect on autophagy, with a slight activation. So, the use of decitabine as an autophagy activator in combination with other drugs could be used as an alternative for current treatments.

Our results showed that use of modulators of autophagy such as metformin, panobinostat, paclitaxel and chloroquine had an inhibiting activity of cellular proliferation. These drugs and decitabin produced changes in cell cycle phases and a deregulation in the autophagic process. According to our preclinical results, these agents could be used in HNSCC in monotherapy or in combination with the current therapies to modify the autophagy mechanisms, an important pathway in these tumours. This synergy could be most appropriate in HPV+ tumours, due to the results from the oropharyngeal squamous carcinoma cell line.

References

1. Sturgis, E. M., Wei, Q. & Spitz, M. R. Descriptive epidemiology and risk factors for head and neck cancer. *Semin. Oncol.* **31,** 726–733 (2004).

2. Siegel, R. L., Miller, K. D. & Jemal, A. Cancer Statistics, 2017. *CA. Cancer J. Clin.* (2016). doi:10.3322/caac.21387

3. Argiris, A., Karamouzis, M. V, Raben, D. & Ferris, R. L. Head and neck cancer. *Lancet (London, England)* **371,** 1695–709 (2008).

4. Marur, S. & Forastiere, A. A. Head and Neck Squamous Cell Carcinoma: Update on Epidemiology, Diagnosis, and Treatment. *Mayo Clin. Proc.* **91,** 386–396 (2016).

5. Leemans, C. R., Braakhuis, B. J. M. & Brakenhoff, R. H. The molecular biology of head and neck cancer. *Nat. Rev. Cancer* **11,** 9–22 (2011).

6. Hermsen, M. *et al.* New chromosomal regions with high-level amplifications in squamous cell carcinomas of the larynx and pharynx, identified by comparative genomic hybridization. *J. Pathol.* **194,** 177–182 (2001).

7. Gollin, S. M. Cytogenetic Alterations and their Molecular Genetic Correlates in Head and Neck Squamous Cell Carcinoma : A Next Generation Window to the Biology of Disease. *Genes Chromosom. Cancer* **0,** (2014).

8. Jin, C. *et al.* Cytogenetic abnormalities in 106 oral squamous cell carcinomas. *Cancer Genet. Cytogenet.* **164,** 44–53 (2006).

9. Ha, P. P. K., Chang, S. S., Glazer, C. A. C., Califano, J. A. J. & Sidransky, D. D. Molecular techniques and genetic alterations in head and neck cancer. *Oral Oncol.* **45,** 335–339 (2009).

10. Chung, C. H. *et al.* Molecular classification of head and neck squamous cell carcinomas using patterns of gene expression. *Cancer Cell* **5,** 489–500 (2004).

11. Lin, C. J. *et al.* Head and neck squamous cell carcinoma cell lines: established models and rationale for selection. *Head Neck* **29,** 163–88 (2007).

12. Glick, D., Barth, S. & Macleod, K. F. Autophagy: Cellular and molecular mechanisms. *Journal of Pathology* **221,** 3–12 (2010).

13. Santana Codina, Naiara, Mancias, Joseph D., Kimmelman, A. C. The role of autophagy in cancer. *Annu. Rev. Cancer Biol.* **1,** 19–39 (2017).

14. Duffy, A., Le, J., Sausville, E. & Emadi, A. Autophagy modulation: A target for cancer treatment development. *Cancer Chemotherapy and Pharmacology* **75,** 439–447 (2015).

15. Cosway, B. & Lovat, P. The role of autophagy in squamous cell carcinoma of the head and neck. *Oral Oncology* **54,** 1–6 (2016).

16. Klionsky, D. J. Autophagy: from phenomenology to molecular understanding in less than a decade. *Nat. Rev. Mol. Cell Biol.* **8,** 931–937 (2007).

17. Sannigrahi, M., Singh, V., Sharma, R., Panda, N. & Khullar, M. Role of autophagy in head and neck cancer and therapeutic resistance. *Oral Dis.* **21,** 283–291 (2014).

18. Klionsky DJ, Abdelmohsen K, Abe A, Abedin MJ, Abeliovich H, Acevedo Arozena A, Adachi H, Adams CM, Adams PD, Adeli K, Adhihetty PJ, Adler SG, Agam G, Agarwal R, Aghi MK, Agnello M, Agostinis P, Aguilar PV, Aguirre-Ghiso J, Airoldi EM, Ait-Si-Ali S, Akemat, Z. S. Guidelines for use and interpretation of assays for monitoring autophagy (3rd edition). *Autophagy* **12,** 1–222 (2016).

19. Sciot, R. *et al.* Inflammatory myofibroblastic tumor of bone: report of two cases with evidence of clonal chromosomal changes. *Am. J. Surg. Pathol.* **21,** 1166–72 (1997).

20. International Standing Committee on Human Cytogenomic Nomenclature, McGowan-Jordan, J., Simons, A. & Schmid, M. (Michael). *ISCN : an international system for human cytogenomic nomenclature (2016)*.

21. Cai, H. *et al.* Progenetix: 12 years of oncogenomic data curation. *Nucleic Acids Res.* **42,** D1055-62 (2014).

22. Bauer, V. L. *et al.* Establishment and Molecular Cytogenetic Characterization of a Cell Culture Model of Head and Neck Squamous Cell Carcinoma (HNSCC). *Genes (Basel).* **1,** 388–412 (2010).

23. Liu, C. J., Lin, S. C., Chen, Y. J., Chang, K. M. & Chang, K. W. Array-comparative genomic hybridization to detect genomewide changes in microdissected primary and metastatic oral squamous cell carcinomas. *Mol. Carcinog.* **45,** 721–731 (2006).

24. Bochen, F. *et al.* Effect of 3q oncogenes SEC62 and SOX2 on lymphatic metastasis and clinical outcome of head and neck squamous cell carcinomas. *Oncotarget* **8,** 4922–4934 (2017).

25. Kimura, T., Takabatake, Y., Takahashi, A. & Isaka, Y. Chloroquine in cancer therapy: A double-edged sword of autophagy. *Cancer Research* **73,** 3–7 (2013).

26. Al-Bari, A. A. Chloroquine analogues in drug discovery: New directions of uses, mechanisms of actions and toxic manifestations from malaria to multifarious diseases. *J. Antimicrob. Chemother.* **70,** 1608–1621 (2014).

27. Pascolo, S. Time to use a dose of Chloroquine as an adjuvant to anti-cancer chemotherapies. *European Journal of Pharmacology* **771,** 139–144 (2016).

28. Park, D. & Lee, Y. Biphasic activity of chloroquine in human colorectal cancer cells. *Dev. Reprod.* **18,** 225–31 (2014).

29. Fan, C., Wang, W., Zhao, B., Zhang, S. & Miao, J. Chloroquine inhibits cell growth and induces cell death in A549 lung cancer cells. *Bioorg Med Chem* **14,** 3218–3222 (2006).

30. Hu, T. *et al.* Chloroquine inhibits hepatocellular carcinoma cell growth in vitro and in vivo. *Oncol. Rep.* **35,** 43–49 (2016).

31. Kalender, A. *et al.* Metformin, independent of AMPK, inhibits mTORC1 in a rag GTPase-dependent manner. *Cell Metab.* **11,** 390–401 (2010).

32. Mizushima, N. The role of the Atg1/ULK1 complex in autophagy regulation. *Current Opinion in Cell Biology* **22,** 132–139 (2010).

33. Yen, Y. C., Lin, C., Lin, S. W., Lin, Y. S. & Weng, S. F. Effect of metformin on the incidence of head and neck cancer in diabetics. *Head Neck* **37,** 1268–1273 (2015).

34. Morales, D. R. & Morris, A. D. Metformin in Cancer Treatment and Prevention. *Annu. Rev. Med.* **66,** 1–13 (2014).

35. Luo, Q. *et al.* In vitro and in vivo anti-tumor effect of metformin as a novel therapeutic agent in human oral squamous cell carcinoma. *BMC Cancer* **12,** 517 (2012).

36. Kato, K. *et al.* The antidiabetic drug metformin inhibits gastric cancer cell proliferation in vitro and in vivo. *Mol Cancer Ther* **11,** 549–560 (2012).

37. Takahashi, A. *et al.* Metformin impairs growth of endometrial cancer cells via cell cycle arrest and concomitant autophagy and apoptosis. *Cancer Cell Int.* **14,** 53 (2014).

38. Barbuti, A. M. & Chen, Z. S. Paclitaxel through the ages of anticancer therapy: Exploring its role in chemoresistance and radiation therapy. *Cancers* **7,** 2360–2371 (2015).

39. Maushagen, R. *et al.* Effects of paclitaxel on permanent head and neck squamous cell carcinoma cell lines and identification of anti-apoptotic caspase 9b. *J. Cancer Res. Clin. Oncol.* **142,** 1261–1271 (2016).

40. Blanchard, P. *et al.* Taxane-cisplatin-fluorouracil as induction chemotherapy in locally advanced head and neck cancers: an individual patient data meta-analysis of the meta-analysis of chemotherapy in head and neck cancer group. *J. Clin. Oncol.* **31,** 2854–2860 (2013).

41. Veldhoen, R. A. *et al.* The chemotherapeutic agent paclitaxel inhibits autophagy through two distinct mechanisms that regulate apoptosis. *Oncogene* **32,** 736–746 (2012).

42. Esteller, M. Epigenetics in cancer. *N. Engl. J. Med.* **358,** 1148–59 (2008).

43. Lane, A. A. & Chabner, B. A. Histone deacetylase inhibitors in cancer therapy. *J. Clin. Oncol.* **27,** 5459–68 (2009).

44. Prince, H. M., Bishton, M. J. & Johnstone, R. W. Panobinostat (LBH589): a potent pan-deacetylase inhibitor with promising activity against hematologic and solid tumors. *Future Oncol.* **5,** 601–12 (2009).

45. Erlich, R. B. *et al.* Preclinical evaluation of dual PI3K-mTOR inhibitors and histone deacetylase inhibitors in head and neck squamous cell carcinoma. *Br. J. Cancer* **106,** 107–15 (2012).

46. Oh, M., Choi, I. K. & Kwon, H. J. Inhibition of histone deacetylase1 induces autophagy. *Biochem. Biophys. Res. Commun.* **369,** 1179–1183 (2008).

47. Ha, P. K. & Califano, J. A. Promoter methylation and inactivation of tumour-suppressor genes in oral squamous-cell carcinoma. *Lancet Oncology* **7,** 77–82 (2006).

48. Derissen, E. J. B., Beijnen, J. H. & Schellens, J. H. M. Concise drug review: azacitidine and decitabine. *Oncologist* **18,** 619–24 (2013).

49. Nieto, M. *et al.* The European Medicines Agency Review of Decitabine (Dacogen) for the Treatment of Adult Patients With Acute Myeloid Leukemia: Summary of the Scientific Assessment of the Committee for Medicinal Products for Human Use. *Oncologist* **21,** 692–700 (2016).

50. Viet, C. T. *et al.* Decitabine rescues cisplatin resistance in head and neck squamous cell

carcinoma. *PLoS One* **9,** e112880 (2014).

Table 1. Autophagy modulator drugs used in this study.

Drug	Trade name	Origin	Concentrations	IC50
Chloroquine	Aralen	Sigma-Aldrich	10, 25, 50, 75, 100, 125µM	25µM
Decitabine	Dacogen	Sigma-Aldrich	0.5, 1, 2, 3, 6, 7.5µM	7.5µM
Metformin	Glucophage	Sigma-Aldrich	0.5, 1, 2.5, 5, 6.5, 8 mM	8mM
Paclitaxel	Taxol	Sigma-Aldrich	2.5, 5, 10, 15, 20, 30nM	10nM
Panobinostat	Farydak	Novartis	10, 25, 50, 75, 100, 150nM	50nM

Table 2. Patient characteristics.

	CAL33	32661	32816	32860
Tumour site	Tongue	Vallecula	Tonsil (oropharynx)	Supraglotis (Larynx)
Sex	Male	Male	Male	Male
Age	69 years	71 years	73 years	68 years
Stage	NA	T4N2b	T3N2b	pT3N1
Tobacco	NA	Yes	Yes	Yes
Alcohol	NA	Yes	Yes	Yes
HPV	NA	Negative	Positive	Negative
Grade	Moderately differentiated	Moderately differentiated	Poorly differentiated	Poorly differentiated

A.

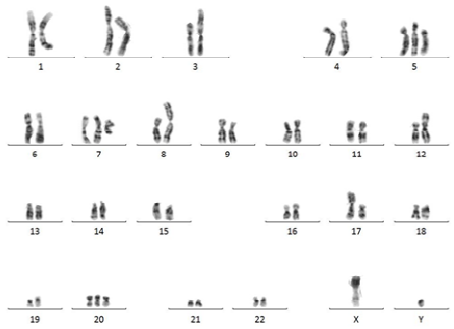

B.

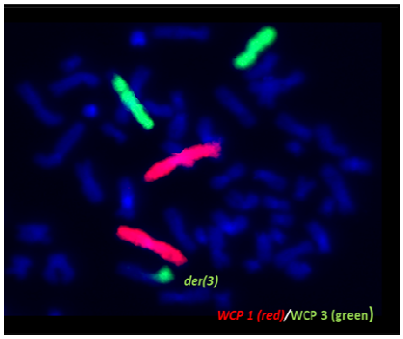

32816 karyotype: 47~49 YY, der(X)add(X)(p?);add(3)(p24),+7,+i(7)p10),i(8)(q10), +del(9)(p11-p24),der(12)t(3;12)(q11;p13),-18,+20 [cp10]

C.

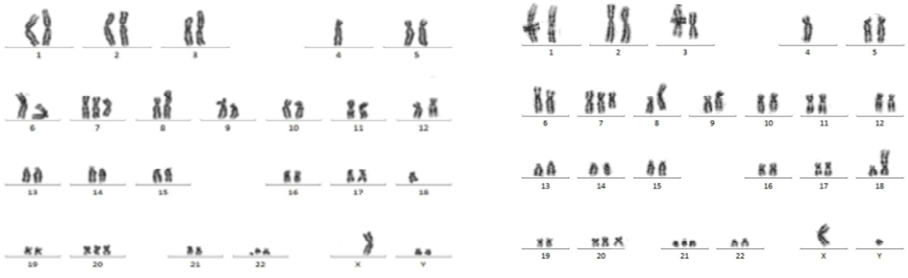

32661 Karyotype: 47~50 YY, der(X)add(X)(p?);add(3)(p24),-4, +i(7)p10), i(8)(q10), del(9)(p11-p24),-18,+20.[cp10]/ 47~50 YY, der(X)add(X)(p?);add(3)(p24),-4, i(7)p10), i(8)(q10), del(9)(p11-p24),der(18)t(18;?)(p11;?),+20 [cp4]

D.

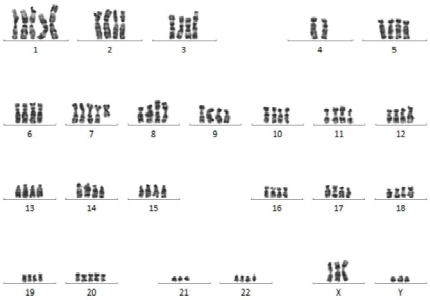

CAL33 karyotype: 96~ YYY, der(x)t(x;?)(p22;?)x3, + der(1)add(1)(p36), der(3)(p25), -4, -4, +i(7)(p10), i(8)(q10)X2, del(9)(p21), -18, +20, -21.

Figure 1. Representative karyotypes of the most different cell lines. A. 32816, C. 32661 and D. CAL33. Figure B demonstrated by FISH analysis the translocation between chromosome 3 and 12.

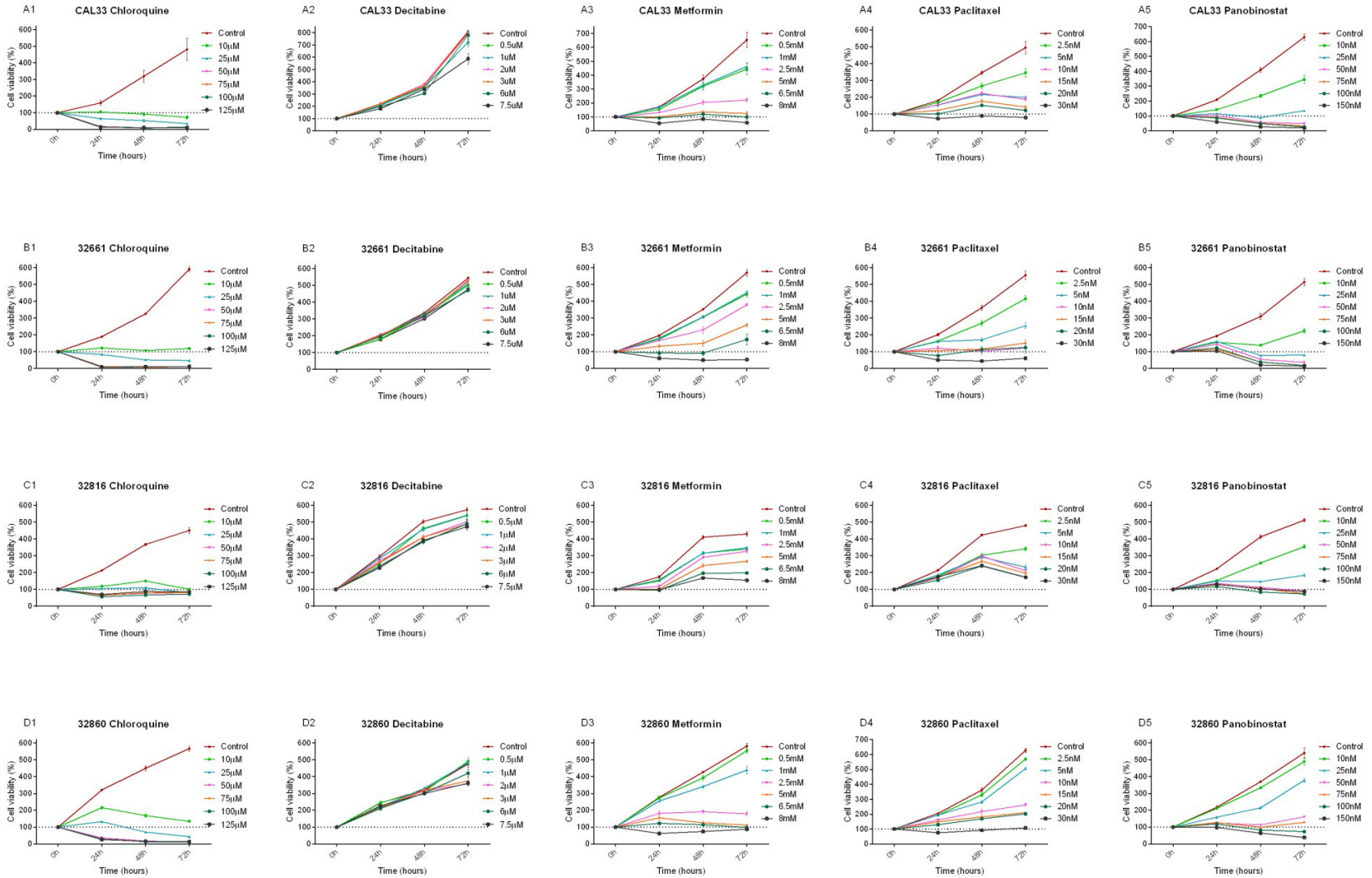

Figure 2. Cell viability graphs by MTT assay during 72 hours. Regarding cell lines A) CAL 33 (tongue), B) 32661 (vallecula), C)32816 (oropharynx), D) 32860 (larynx) and respect to drug treatment 1) chloroquine, 2) decitabine, 3) metformin, 4) paclitaxel and 5) panobinostat. Different drug concentrations are represented by different colours indicated in the right side of the graph. Control untreated cell line shows the normal viability. Y axis represents percentage of cell viability while X axis shows each 24 hours treatment for three days.

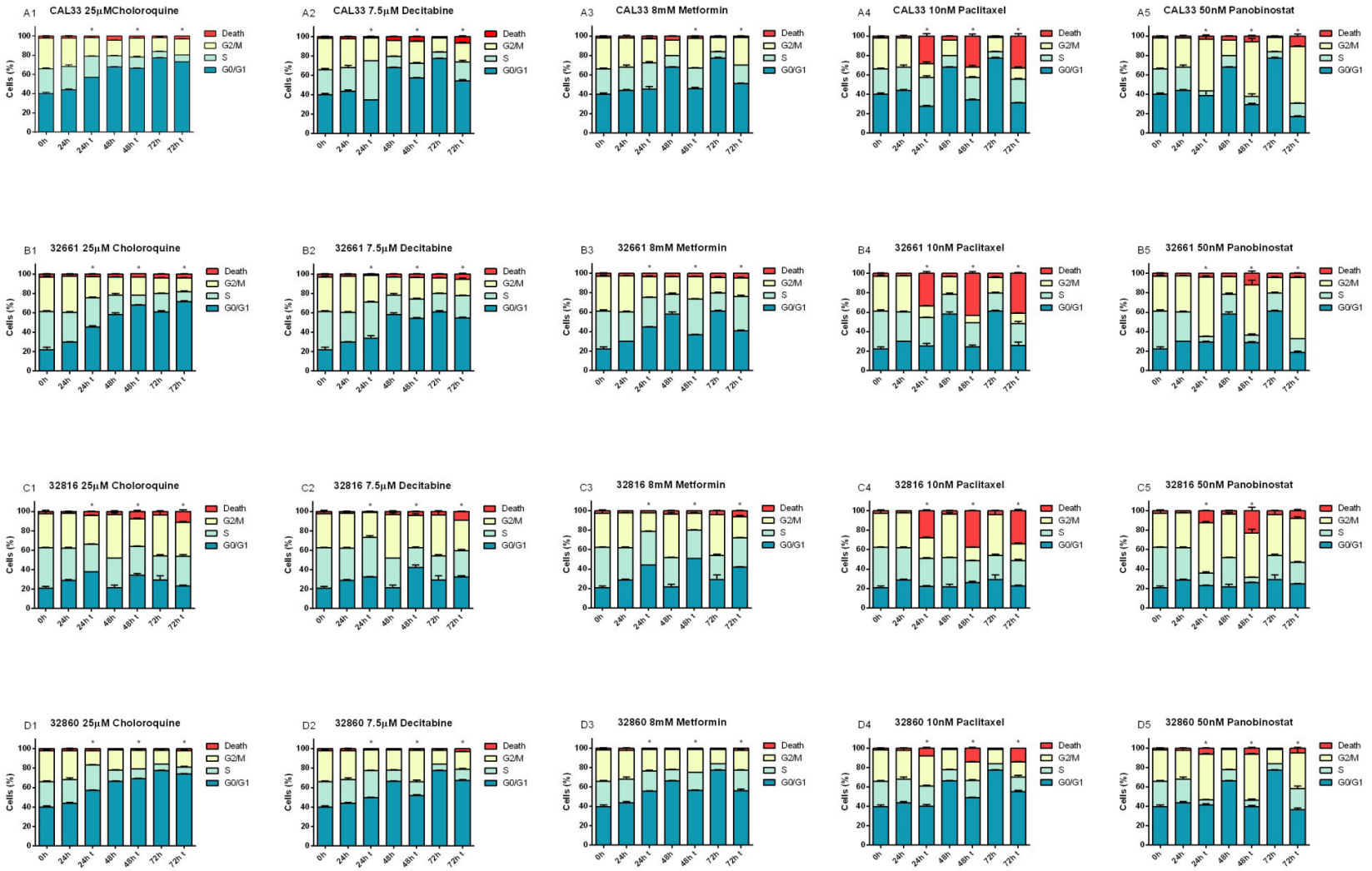

Figure 3. Cell cycle phase by flow cytometry assay during 72 hours in untreated and treated (t) cell cultures. Regarding cell lines A) CAL33 (tongue), B) 32661 (vallecula), C) 32816 (oropharynx), D) 32860 (larynx) and respect to drug treatment 1) 25µM chloroquine, 2) 7.5µM decitabine, 3) 8mM metformin, 4) 10nM paclitaxel and 5) 50 nM panobinostat. Cell cycle phases are indicated by different colours (right side of the graph). Y axis represents percentage of cell cycle phase while X axis shows each 24 hours treatment for three days. Statistically significant results respect the untreated controls are indicated by an asterisk.

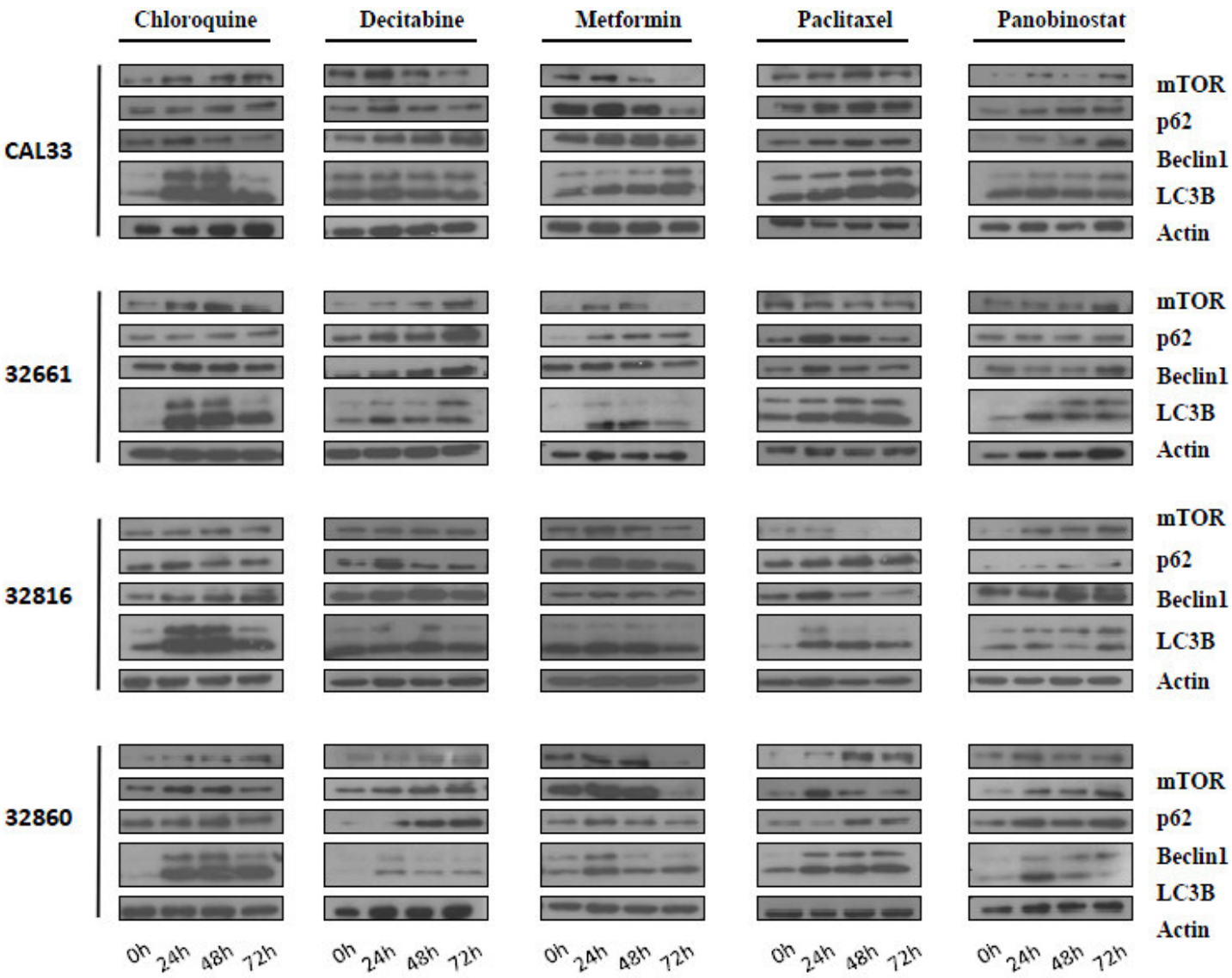

Figure 4. Western blot of autophagy related proteins: phosphor-mTOR, p62, beclin1 and LC3B (I and II). Actin served as a loading control. We show the effect after the treatment with different autophagy modulators during 72 hours in each HNSCC cell line.

Supplementary table S1. Karyotypes and chromosomal regions of DNA copy number aberrations detected by aCGH in four HNSCC cell lines.

Type Cell Line	Copy Number Changes Detected by array CGH		Karyotype
	Gains	Losses	
LC_32661	3q11.1-3q29,7p23.3-7p11.2, 8q12.1 8q24.3, 9p24.3-p22.2, 9p13.3-9q22.33, 9q31.1-9q31.3, 9q34, 14q32.33,16p13.3-16p11.2, 18q12.3, 20p13-q13.33, Xp22.2-p22.12	2p25.2-2p13.3, 3p14.3-3p11.1, 4p15, 4p14, 4p13, 4q12, 4q13.3, 4q21.1-q34.1, 4q34.3-4q35.2, 8p23.3-8p12, 8p11.23, 12q24.31-q24.33, 18q12.1, 18q12.2-18q12.3, 18q12.3-18q23, Xp22.33-p22.31	47~50 YY, der(X)add(X)(p?);add(3)(p24),-4, +i(7)p10), i(8)(q10), del(9)(p11-p24),-18,+20.[cp10]/ 47~50 YY, der(X)add(X)(p?);add(3)(p24),-4, i(7)p10), i(8)(q10), del(9)(p11-p24),der(18)t(18;?)(p11;?),+20 [cp4]
LC_32816	3q11.1-q29, 7p23.3-p11.2, 8q13.1-q24.3, 9p24.3-p22.2, 9q13-34.13, 9q34.2-q34.3, 16p13.33-p11.2, 20p13-q11.2, 20q11.2-q13.33, Xp22.2-p22.12, Yp11.31-p11.2, Yp11.2-q11.23	3p21.1-p11.2, 4q34.3-q35.2, 8p23.3-8p22, 8p21.3-8p21.1, 8p12, 12p13.33, 12q24.31-q24.33, 16q22.1,18p11.21-q11.1, 18q11.2-q23	47~49 YY, der(X)add(X)(p?);add(3)(p24),+7,+i(7)p10),i(8)(q10), +del(9)(p11-p24),der(12)t(3;12)(q11;p13),-18,+20 [cp10]
LC_32860	3q11.1-q13.33, 3q13.33-q27.3, 3q27.3-3q29, 7p23.3-p15.2, 7p15.2-p14.1, 7p14.1-p11.2, 8p11-18q24.3, 9p24.3-p23, 9p23-p22, 9p13.3q21.13, 9q21.13-q22.33, 9q31.1-q31.3, 9q34,16p13.3-p11.2, 18q12.3, 20p13-q11.22, 20q11,22-q13.33, Xp22.31-p22.2, Xp22.2-p22.13	3p26.3-p11.1, 4q34.3-q35.2, 8p23.3-p11.1, 12q24.31-q24.33, 16q22.1,18q12.2-q12.3,18q12.3-q21.31, 18q21.31-q23	47~49 YY, der(X)add(X)(p?);add(3)(p24),+7, +i(7)p10), i(8)(q10), del(9)(p11-p24), -18,+20
LC_CAL33	3q11.2-q29, 7p22.3-p15.2, 7p15.2-p11.2, 8p11.1-8q24.3, 9p24.3-p24.1, 9p13.1-q34.3,13q12.1-q13.3, 13q14.11, 13q14.12-, 13q14.3, 13q21.1, 13q21.33, 13q31.1, 13q31.3,13q32.3, 13q32.3, 13q33.2-q33.3, 16p13.3-p11.2, 20p13-q11.22, 20q11.2-q13.33, Xp22.31-p22.12	3p26.3-p36.1, 3p35.3, 3p25.1, 3p24.3, 3p23, 3p22, 3p21.31, 3p14.2, 3p14.1, 3p12.1, 4p15.33, 4p15.2, 4p14, 4q13.3, 4q22.1, 4q25, 4q28.2, 4q31.3, 4q34.3-q35.1, 5p15.33-p15.2, 5p12.2, 5p13, 5q12.1, 5q13.3,5q14.3,5q21.1, 5q23.1, 5q33.1-q33.3, 5q35, 8p23.3-p23.1, 8p22, 8p21.3, 8p12, 8p11.21, 12q24.31-q24.33, 16q22.1, 18q11.2, 18q12.1, 18q12.2, 18q12.3, 18q21.2, 18q22.1-q23, 21q21.1-q21.3, 21q21.3, 21q22.3	96~ YYY, der(x)t(x;?)(p22;?)x3, + der(1)add(1)(p36), der(3)(p25), -4, -4, +i(7)(p10), i(8)(q10)X2, del(9)(p21), -18, +20, -21.

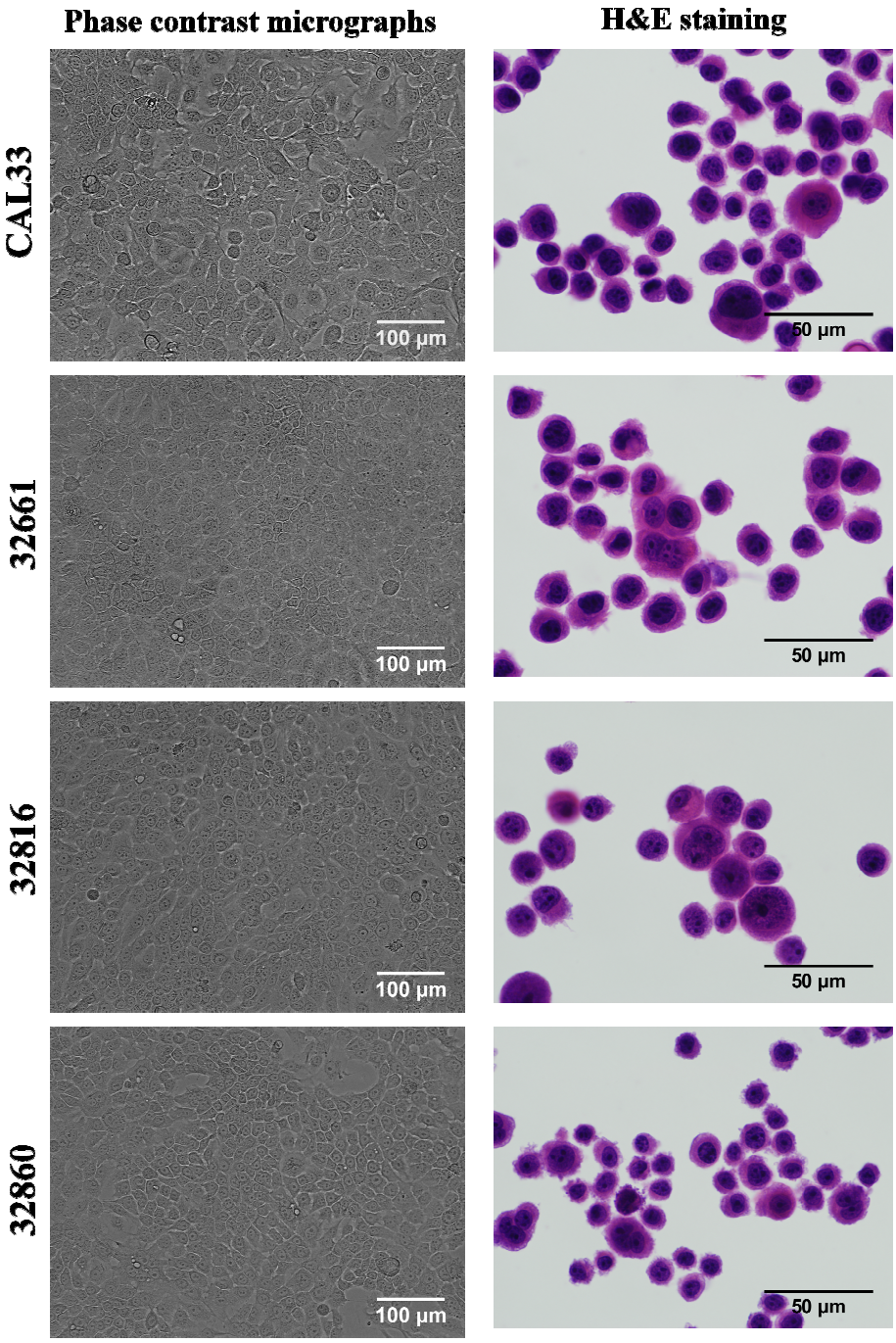

Supplementary figure S1. Phase contrast microscope photographs and H&E from the commercial cell line CAL33 and the established cell lines 32661, 32816 and 32860.

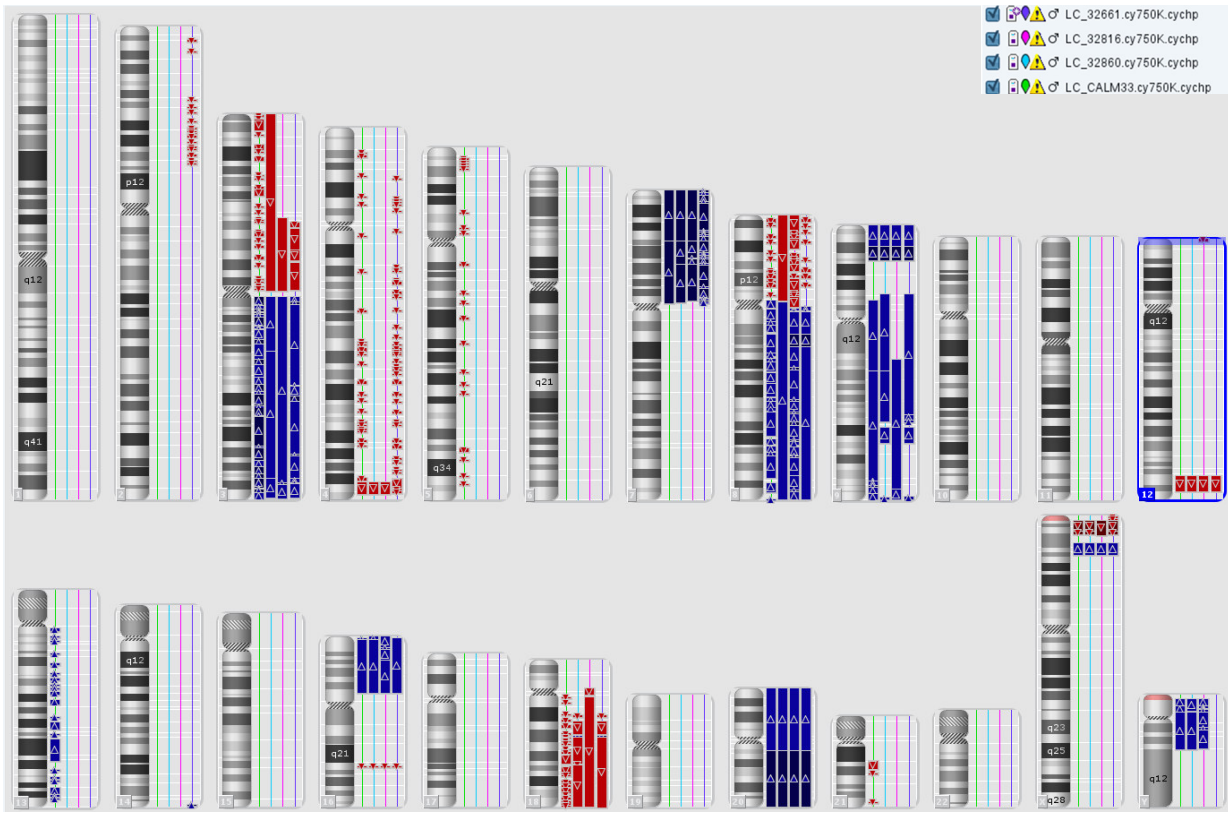

Supplementary figure S2. – Whole genomic array CGH profile of the four HNSCC cell line. Karyoview of identified genomic abnormalities (right of each ideogram). Gains are shown in blue bars (regions of CN2–3 in light blue and CN≥3 in dark blue). Losses are shown analogically in red bars (regions of CN1–2 in light red and CN≤1 in dark red). Green line represents tongue carcinoma cell line CAL33, light blue laryngeal cell line 32860, pink oropharyngeal carcinoma cell line 32816 and purple vallecula cell line 32661.